

Detection of Symmetrical Faults by Distance Relays During Power Swings

Saeed Lotfifard, *Student Member, IEEE*, Jawad Faiz, *Senior Member, IEEE*, and Mladen Kezunovic, *Fellow, IEEE*

Abstract—For maintaining security of distance relays, power swing blocking is necessary to prevent unintended operation under power swings. To be dependable, distance relays must operate whenever a fault occurs. Therefore, detecting faults during power swings is an important issue since the relay should be able to differentiate the fault condition and not be blocked during that time. This paper presents a new method for detecting a symmetrical fault during a power swing, based on extracting components of the current waveform using the Prony method. The merit of the method is demonstrated by simulating different faults during power swing conditions using the Alternate Transients Program version of the Electromagnetic Transients Program.

Index Terms—Distance relay, power swing, prony method, symmetrical fault.

I. INTRODUCTION

DISTANCE relay used for transmission line protection is designed to trip if the line faults occur within the specified zone. It is not supposed to trip during the power swing caused by the disturbances outside the protected line [1]. In order to avoid an unintended operation, power swing blocking function is used.

Conventional power swing blocking method is based on timing the movement of the measured impedance through the zones of the relay. During the fault conditions calculated (apparent) impedance moves along the locus almost instantaneously. However, under power swing conditions the impedance moves slowly, typically takes hundreds of milliseconds before approaching the relaying zones. The time delay for discriminating fault from power swing has to be set with knowledge of the likely speed of movement of the impedance during the power swing, so it is possible that relay fails to block if the apparent impedance moves too fast. Moreover, the relay may not respond to genuine faults occurring during the power swing period since it is blocked from operation [2], [3]. This will inevitably delay the operation of relay when a fault occurs during the power swings. Therefore, fault detection during power swing is an important issue [4].

Presence of negative and zero sequence components due to asymmetrical faults, which do not exist during the stable power

swing, makes it possible to detect fault during the power swing. However, there are no such components during symmetrical fault. Some symmetrical fault detectors are based on the superimposed components or the rate-of-change of measured impedance. The issue related to these methods is inability to operate sensitively for the faults that cause very small superimposed components, such as the ones that happen at the power swing center and the power angle close to 180° [5].

Magnitude of the swing-center voltage (SCV), defined as the voltage at the location of a two-source equivalent system where the voltage value is zero and the angles between the two sources are 180° apart, is used to distinguish faults from power swing [6]. However, it is difficult to set the threshold, especially when a fault arc is considered.

In [7] and [8], a method based on the monitoring of the voltage phase angle at the relay location is proposed to discriminate fault from power swing. Only the single-phase faults have been simulated and the method has not been applied to symmetrical faults [9].

In [10], an adaptive neuro-fuzzy inference systems (ANFIS) based method has been proposed. The method needs a huge number of training patterns to be produced by simulations of various cases. Moreover, it might need re-training for use in different power systems.

A wavelet-based signal processing technique is an effective tool for power system transient analysis and feature extraction [11], [12]. In [9], the wavelet transform (WT) has been utilized for detecting fault during the power swing. It is based on the presence of high frequency signal components created at the inception of the fault. The implementation needs high frequency sampling.

This paper presents a new symmetrical fault detector for distance relay that avoids the disadvantages of previous schemes while it maintains the required selectivity. This detector is based on the extraction of the current waveform components using the Prony method, which is briefly described first. Proposed algorithm that detects faults by monitoring the presence of decaying dc in current waveform is discussed next. Finally, the performance of the proposed scheme is studied by simulating various faults and power swing cases using ATP version of EMTP.

II. PRONY METHOD

The Prony method is a tool that has been used in signal processing applications and recently has been introduced to the power system protection field [13], [14]. This method is considered a powerful tool for analyzing a signal and extracting its modal information. The fact that the Prony can handle damped signals and estimate the damping coefficient makes it suitable for applications based on properties of power system transients.

Manuscript received June 09, 2009. First published December 08, 2009; current version published December 23, 2009. Paper no. TPWRD-00071-2009.

S. Lotfifard and M. Kezunovic are with the Department of Electrical and Computer Engineering, Texas A&M University, College Station, TX 77843-3128 USA (e-mail: s.lotfifard@neo.tamu.edu; keza@verizon.net).

J. Faiz is with the Center of Excellence on Applied Electromagnetic Systems, School of Electrical and Computer Engineering, University of Tehran, Tehran 1439957131, Iran (e-mail: jfaiz@ut.ac.ir).

Digital Object Identifier 10.1109/TPWRD.2009.2035224

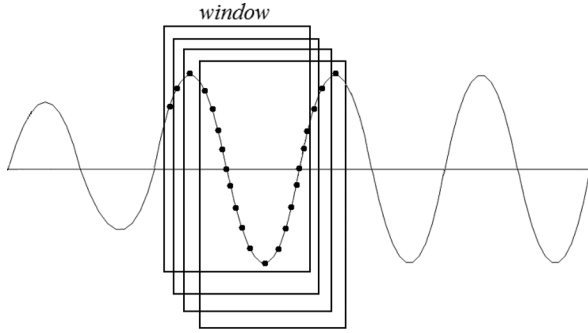


Fig. 1. Sliding data window.

Prony calculates the modal information, such as frequency, amplitude, damping, and phase shift; these can be used to reconstruct the original signal or to make inferences about the system conditions that affected the signal. The fact that Prony can be used for system stability and protection purposes makes it a good candidate for the modern concept of wide-area protection and emergency control [15].

The Prony analysis directly estimates the parameters of the uniformly sampled signal by fitting a sum of complex damped sinusoids as follows:

$$y(t) = \sum_{i=1}^N A_i e^{(-\sigma_i t)} \cos(2\pi f_i t + \phi_i) \quad (1)$$

- A_i amplitude of component i ;
- σ_i damping coefficient of component i ;
- ϕ_i phase of component i ;
- f_i frequency of component i ;
- N total number of damped exponential components.

The Prony problem is formulated by knowing the value of the signal $y(t)$ in the form of a series of time samples. The problem is solved to estimate the value of parameters of the Prony method such that the squared errors of the fit are minimized. The mathematical details explaining the approach have been reported in [16].

In order to calculate waveform components from the relay point of view, windowed-Prony method is used. Fig. 1 shows this approach. Waveform components are calculated in each window and they are updated as a new sample comes and the oldest gets dropped. Using shorter window makes the process faster but reduces the accuracy. The window should be short enough to achieve reasonable speed and long enough to reach desired accuracy.

Fig. 2 shows the estimated amplitude of fundamental component of the following signal with different data window lengths:

$$i(t) = \begin{cases} \text{Sin}(\omega t) & t \leq 0.3 \\ e^{(-5t)} + 10\text{Sin}(\omega t) + 3\text{Sin}(2\omega t) & t \geq 0.3 \end{cases} \quad (2)$$

Although half a cycle window is faster, it has abrupt changes during transient conditions. Two-cycle window has a long delay. One cycle window does not have such a delay, while it does not

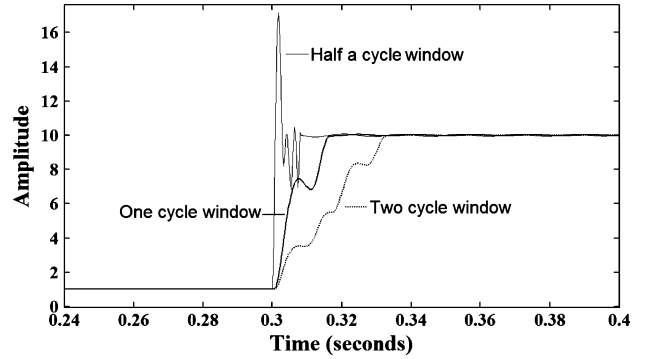


Fig. 2. Estimated amplitude of fundamental component with different data window lengths.

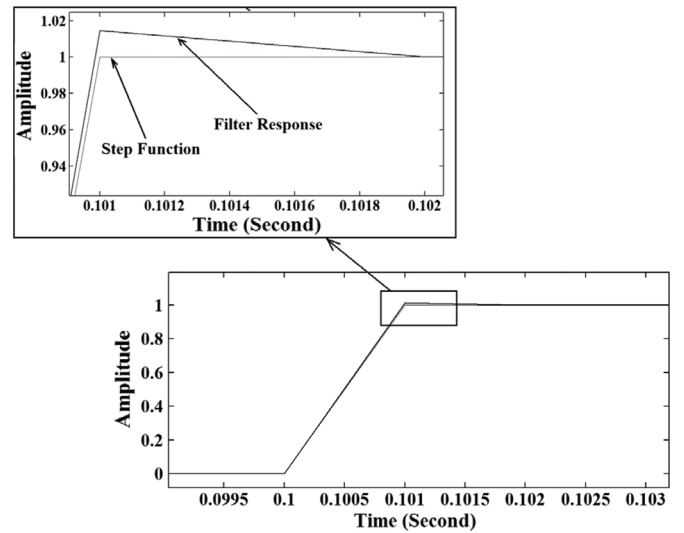


Fig. 3. Step response of second order Butterworth low pass filter with cut off frequency of 1 kHz.

change too abruptly like half a cycle window. As a result, in this paper one cycle is chosen for data window length.

As the proposed method is not based on high frequency component of signal, it does not need very high sampling frequency. Therefore, sampling frequency of 3 k Hz (50 samples per cycle) is selected which means interval between two samples in Fig. 1 is 0.33 ms.

In order to avoid aliasing phenomena in processing of the signal, anti aliasing filter is used [17]. To satisfy the Nyquist criterion, frequencies higher than one-half of the sampling frequency should be removed from the signal. It means cut-off frequency (-3 dB) of the anti aliasing filter should be set at less than half a sampling frequency. In practice, such a filter cannot remove all unwanted frequencies, so the cut-off frequency of the filter is set at about one third of the sampling frequency [18]. The anti aliasing filter selected in this paper, is Butterworth low pass filter which is used commonly in protective relaying [19] Fig. 3 shows step response of the second order Butterworth low pass filter with cut-off (-3 dB) frequency of 1 kHz.

III. PROPOSED ALGORITHM

Fig. 4 shows a typical current waveform during a power swing. During power swings in a two-machine system, the

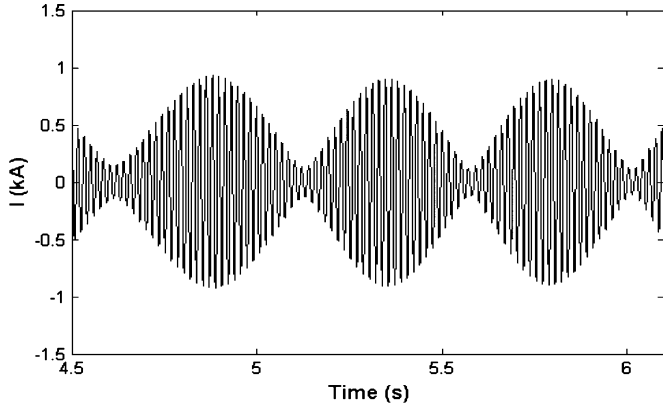


Fig. 4. Typical current waveform during power swing.

current in the transmission lines is composed of two sinusoidal components that can be given as follows:

$$i(t) = I_1 \sin(2\pi f_1 t + \varphi_1) + I_2 \sin(2\pi f_2 t + \varphi_2) \quad (3)$$

where I_1 , I_2 are the amplitudes of the two sinusoidal components, f_1 , f_2 are the two unknown frequencies and φ_1 , φ_2 are the initial phase angles.

It is easily shown that the following equation holds for adding two sine functions:

$$A \sin(\omega t) + B \sin(\omega t + \alpha) = C \sin(\omega t + \varphi) \quad (4)$$

where

$$C = \sqrt{A^2 + B^2 + 2AB \cos(\alpha)} \quad (5)$$

$$\sin(\varphi) = \frac{B \sin(\alpha)}{C} \quad (6)$$

$$\cos(\varphi) = \frac{A + B \cos(\alpha)}{C}. \quad (7)$$

Using the (4)–(7), (3) can be written as follows:

$$i(t) = I_1 \sin(2\pi f_1 t + \varphi_1) + I_2 \sin(2\pi f_2 t + \varphi_2) = I \sin(2\pi f_1 t + \varphi). \quad (8)$$

I is obtained according to (5) by substituting A and B with I_1 and I_2 respectively. φ is yielded by solving (6) and (7) in which δ is $(2\pi(f_2 - f_1)t + \varphi_2 - \varphi_1)$.

If I_1 is almost equal to I_2 , which usually is the case, (3) can be written in a simpler form. Assuming that $I_1 = I_2 = I$, the current signals can be written as follows:

$$i(t) = 2I \cdot \cos(2\pi t(f_1 - f_2)/2 + \Theta_1) \cdot \sin(2\pi t(f_1 + f_2)/2 + \Theta_2) \quad (9)$$

where $(f_1 - f_2)/2$ is the frequency of the current envelope and $(f_1 + f_2)/2$ is the mean frequency of the sampled current. Θ_1 is $(\varphi_1 - \varphi_2)/2$ and Θ_2 is $(\varphi_1 + \varphi_2)/2$ [20]. Equations (8) and (9) express Fig. 4 in mathematical form, which is a sinusoidal waveform with modulated amplitude that varies with time.

Fig. 5 shows the Thevenin equivalent of a fault in a power system. Applying Kirchhoff's voltage law leads to the following differential equation [21]:

$$E_{\max} \sin(\omega t + \varphi) = Ri + L \frac{di}{dt} \quad (10)$$

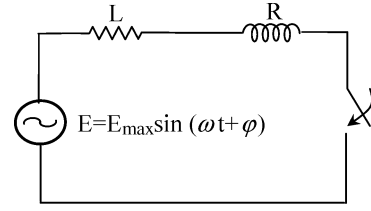


Fig. 5. Thevenin equivalent of a faulted system.

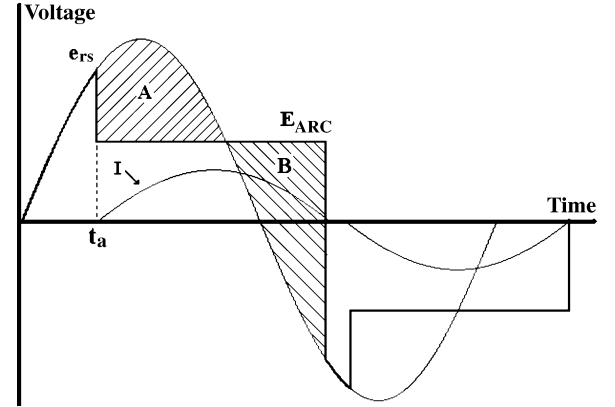


Fig. 6. Voltage and current conditions during the first 1/2 cycle after arc initiation.

By solving (10), the current will be as follows:

$$i(t) = e^{-(\frac{R}{L})t} \left\{ \frac{-E_{\max}}{\sqrt{R^2 + \omega^2 L^2}} \sin \left[\varphi - \tan^{-1} \left(\frac{\omega L}{R} \right) \right] \right\} + \frac{-E_{\max}}{\sqrt{R^2 + \omega^2 L^2}} \sin \left[\omega t + \varphi - \tan^{-1} \left(\frac{\omega L}{R} \right) \right]. \quad (11)$$

It is well known that power systems are exposed to faults involving arc phenomena. The arc current can be described using the process presented in [22]. According to Fig. 6 [22] which shows the arc voltage and current, after arc initiation, the first voltage zero crossover occurs at $t = 0$. Beginning at this point the voltage across the arc equals the system driving voltage.

When the voltage reaches the value e_{rs} , the arc will re-strike and the voltage will quickly decrease to the arc voltage E_{ARC} . Current, i , will begin to flow in the circuit and will increase as long as the driving voltage, e , exceeds E_{ARC} . When $e = E_{ARC}$, the current is at its maximum and it will begin to decrease. The current is mathematically proportional to the volt-time area A minus volt-time area B for any time t .

When the volt-time area A equals to the volt-time area B , as shown by the shaded area in Fig. 6, the current will be zero, the arc will extinguish, and the arc voltage will quickly be equal to the driving voltage again. If the driving voltage at this point is equal or larger than e_{rs} the arc re-strikes immediately and the current wave becomes sinusoidal, so amplitude and shape of the arc current become identical to those of the short-circuit current [23]. But if it is below e_{rs} , the arc will not re-strike. When the voltage across the arc reaches e_{rs} once again the arc will re-strike on the negative half cycle which will be a mirror image of the positive half cycle [22].

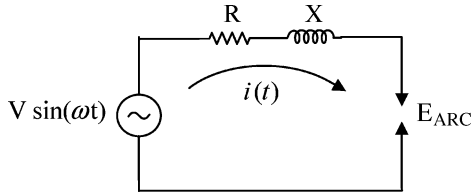


Fig. 7. Thevenin equivalent of faulted circuit with arc included.

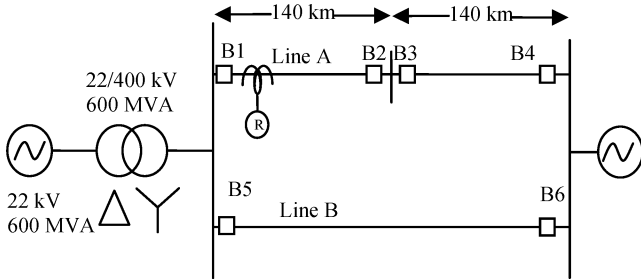


Fig. 8. Schematic of a simulated power system.

A mathematical expression for the arc current can be derived using the Thevenin equivalent circuit of electrical system with the arc included, as shown in Fig. 7 [22]. Current $i(t)$ can be calculated as follows:

$$i(t) = \begin{cases} 0 & t \leq t_a \\ \frac{V}{Z} \left[\sin(\omega t - \alpha) - e^{-\frac{R}{X}\omega(t-t_a)} \sin(\omega t_a - \alpha) \right] & t \leq t_a \\ -\frac{E_{ARC}}{R} \left(1 - e^{-\frac{R}{X}\omega(t-t_a)} \right) & t \geq t_a \end{cases} \quad (12)$$

where

- α $\arctan(X/R)$;
- Z System impedance $= R + jX$;
- X system inductive reactance;
- R system resistance.

According to (8), (9), (11) and (12), fault current comprises a decaying dc part, while there is no such a part in current waveform during pure power swing. Therefore, presence of decaying dc in current waveform can be used as a sign for detecting fault.

It is noticeable that if in (11) $\varphi = \tan^{-1}(\omega L/R)$, then there is no decaying dc in the current waveform in the phase under study. As there is 120 degrees phase shift between different phases in three-phase system, there is a decaying dc in other phases. The presence of decaying dc at least in one phase implies that the fault has occurred and the relay must be unblocked.

IV. SIMULATION RESULTS

To investigate the merit of the proposed algorithm, a power system shown in Fig. 8 [9] is modeled using ATP version of EMTP. The system details have been given in [9].

The distance relay located at breaker B1 is considered here. A fault happens at 0.1 s on Line-B and is cleared 0.08 s later by opening breakers B5 and B6. This causes the system to go into a power swing. Three-phase faults are now simulated at various locations on line-A at different time instants.

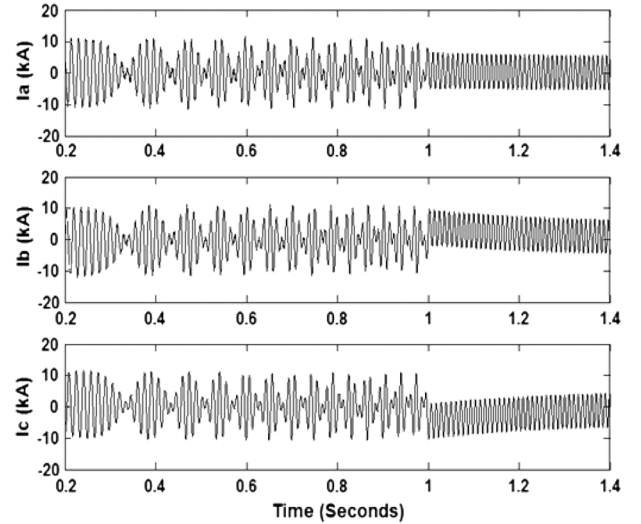


Fig. 9. Current waveforms due to three-phase fault.

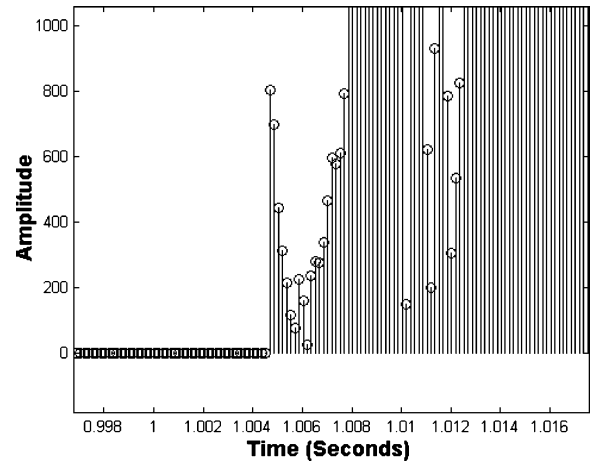


Fig. 10. Amplitude of decaying dc versus time during three-phase fault.

Since the method depends on the relationship between faults and occurrence of decaying dc component in the signals, this behavior should be investigated and demonstrated. The decaying dc component depends on many factors in the network and hence it needs to be shown that the scheme is selective under all such factors. The time constant and amplitude of the decaying dc are unknown and depend on the fault resistance, fault position and the fault incipient time [24]. The effect of these factors was studied and in all cases the selectivity of the proposed method was proven.

Detailed studies of two typical cases and results of some other cases are presented below and in Table III.

In the first case, a three-phase fault with $Z_f = 5 \Omega$ happens at time instant of 1 s, distance of 30 km from the relay and pre-fault power angle of $\delta = 60$ degrees. Fig. 9 shows currents due to the three-phase fault.

Fig. 10 shows amplitude of decaying dc component of the current waveform of phase c at each time window. It is clear that amplitude of decaying dc component increases after inception of the fault.

TABLE I
CURRENT WAVEFORM COMPONENTS DURING THREE-PHASE FAULT AND POWER SWING

	Ia			Ib			Ic		
	Amplitude	Frequency	Damping	Amplitude	Frequency	Damping	Amplitude	Frequency	Damping
Three Phase Fault	5.5e ³	5.9e ¹	1.1e ⁻²	7.3e ³	0	4.5	7.8e ³	0	1.5
	7.4e ²	0	5.7e ⁻¹	5.5e ³	6.0e ¹	2.9e ⁻¹	5.4e ³	6.0e ¹	6.5
	4.5e ²	1.2e ²	0.3e ¹	4.5e ²	1.2e ²	2.4	4.5e ²	1.2e ²	3.1
	1.2e ²	5.1e ²	1.7e ⁻¹	7.7e ¹	5.1e ²	1.7e ⁻¹	4.7e ¹	5.1e ²	1.7e ⁻¹
	8.5	6.9e ²	1.6e ¹	8.6	6.9e ²	1.6e ¹	8.5	6.9e ²	1.6e ¹
	1.8	3.2e ²	4.4e ¹	8.9e ⁻¹	3.2e ²	1.7e ⁻¹	2.2	7.7e ²	1.7e ³
	8.9e ⁻²	5.7e ²	6.8e ²	2.8e ⁻¹	1.3e ³	6.4e ²	1.2	3.3e ²	3.8e ¹
	7.5e ⁻²	9.7e ²	3.2e ²	6.4e ⁻²	1.4e ³	2.2e ²	3.7e ⁻¹	5.4e ²	7.2e ²
	6.7e ⁻²	1.3e ³	3.9e ²	6.3e ⁻²	1.2e ³	2.3e ²	2.9e ⁻¹	8.4e ²	5.9e ²
	5.6e ⁻²	8.4e ²	2.0e ²	3.9e ⁻²	1.1e ³	2.7e ²	5.9e ⁻²	1.4e ³	1.6e ²
Power Swing	6.3e ³	8.9e ¹	1.7e ⁻¹	9.2e ³	8.4e ¹	3.4e ⁻¹	8.0e ³	6.7e ¹	2.2
	6.2e ³	6.2e ¹	0.8e ⁻¹	5.0e ³	5.6e ¹	2.2e ⁻¹	3.9e ³	9.1e ¹	2.8e ¹
	5.4e ²	4.5e ²	2.2e ⁻¹	4.4e ²	4.5e ²	2.1e ⁻¹	1.1e ²	4.5e ²	2.6e ⁻¹
	9.6e ¹	2.0e ²	1.1e ³	2.1e ²	1.4e ²	1.2e ²	3.2e ¹	2.8e ²	1.3
	3.2e ¹	2.8e ⁻²	2.1	4.2e ¹	2.4e ²	1.1e ³	2.8e ⁻¹	6.1e ⁻²	2.5e ⁻¹
	2.7e ¹	6.2e ²	8.9e ⁻¹	3.2e ¹	2.8e ²	4	1.2e ¹	1.3e ³	2.1
	2.0e ¹	1.5e ²	5.2e ¹	2.7e ¹	6.2e ²	1.1	1.1e ¹	1.6e ²	6.6e ¹
	1.5e ¹	1.3e ³	2.2	1.7e ¹	1.3e ³	2.1	1.7	1.2e ³	2.5
	1.4	1.2e ³	9.4e ⁻¹	1.4	1.2e ³	1.5	8.4e ⁻¹	1.5e ³	2.6e ³
	0.9	9.4e ²	1.2e ³	4.3e ⁻¹	1500	1.3e ⁻¹	5.0e ⁻²	6.2e ²	5.6

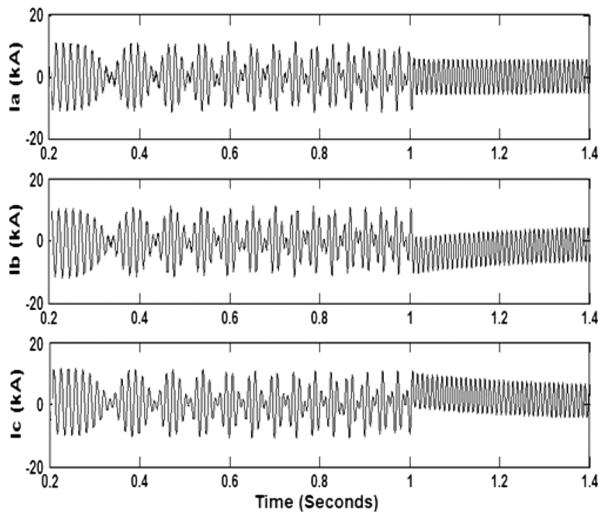


Fig. 11. Current waveforms due to three-phase fault while arc is included.

Table I shows current waveform components during one data window for three-phase fault and power swing.

The values have been shown in the order of the amplitude values.

In Table I, the values are components of current waveforms during one data window (50 samples) of the signal. For instance for Ia, in presence of three-phase fault, components that build up the current waveform in that interval (one window) are as follow: a sine function with frequency of 59 Hz (≈ 60 Hz) with amplitude of $5.5e^3$ and damping of $1.1e^{-2}$ (refer to (1)) and decaying dc (frequency of 0) with amplitude of $7.4e^2$ and damping of $5.7e^{-1}$ and so on.

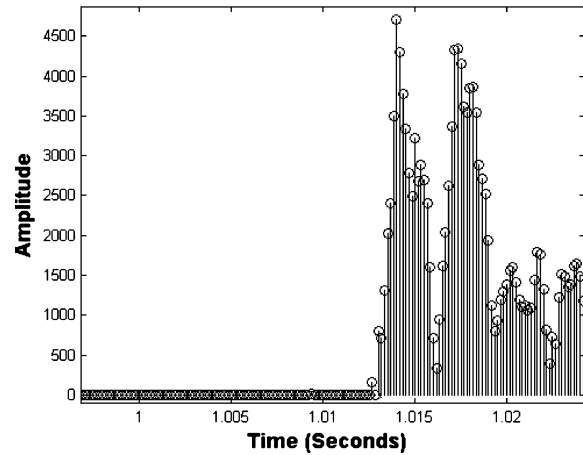


Fig. 12. Amplitude of decaying dc versus time during three-phase fault including arc.

TABLE II
CURRENT WAVEFORM COMPONENTS DURING THE THREE-PHASE FAULT WHILE ARC IS INCLUDED AND POWER SWING

	Ia			Ib			Ic		
	Amplitude	Frequency	Damping	Amplitude	Frequency	Damping	Amplitude	Frequency	Damping
Three Phase Fault	5.4e ³	60e ¹	8.4e ⁻²	8.4e ³	0	4.0	8.1e ³	0	4.1
	5.4e ²	0	9.3e ⁻¹	5.4e ³	61e ¹	1.6e ⁻¹	5.4e ³	59e ¹	0.2
	4.8e ²	1.2e ²	9.9e ⁻¹	4.6e ²	1.2e ²	1.4	4.8e ²	1.8e ²	1.4
	1.8e ²	5.1e ²	1.7e ⁻¹	3.7e ²	5.7e ¹	6.2e ²	7.2e ¹	5.1e ²	1.7e ⁻¹
	2.0e ¹	2.9e ²	1.1e ³	9.7e ¹	5.1e ²	1.7e ⁻¹	1.3e ¹	6.9e ²	1.7e ⁻¹
	1.3e ¹	6.9e ²	1.7e ⁻¹	1.2e ¹	6.9e ²	1.9e ⁻¹	2.4	3.2e ²	4.2e ¹
	3.2	5.8e ²	8.3e ²	18	4.0e ²	5.0e ²	1.1e ⁻¹	7.6e ²	2.1e ²
	1.4	3.2e ²	7.0	9.4e ⁻¹	3.1e ²	2.6e ⁻¹	5.7e-3	1.2e ³	1.1e ²
	7.1e ⁻¹	7.6e ²	4.1e ²	8e ⁻¹	9.9e ²	1.2e ³	3.7e-3	1.4e ³	3.5e ²
	7.2e ⁻²	1.5e ³	2.7e ²	1e ⁻¹	1.4e ³	3.7e ²	1.2e-3	1.0e ³	1.6e ²
Power Swing	6.7e ³	6.3e ¹	1.5e ⁻¹	9.7e ³	9.6e ¹	7.1e ⁻¹	8.9e ³	8.1e ¹	3.3e ¹
	6.5e ³	8.8e ¹	2.4e ⁻¹	4.0e ³	6.1e ¹	1.3e ⁻¹	2.8e ³	5.3e ¹	6.5
	5.4e ²	4.5e ²	2.4e ⁻¹	4.3e ²	4.5e ²	2.6e ⁻¹	1.1e ²	4.5e ²	2.5e ⁻¹
	3.5e ¹	1.5e ²	5.3	1.5e ²	1.8e ²	1.4e ³	3.5e ¹	1.4e ²	1.2e ¹
	3.2e ¹	2.8e ²	1.9	3.1e ¹	2.7e ²	5.6e ⁻¹	3.1e ¹	2.8e ²	1.7
	2.7e ¹	6.1e ²	4.6	2.7e ¹	6.2e ²	2.1e ⁻¹	2.6e ¹	6.2e ²	1.5
	1.5e ¹	1.3e ³	2.1	1.5e ¹	1.3e ³	2.2	1.4e ¹	1.3e ³	2.2
	2.0	5.6e ²	1.0e ³	5.9	1.5e ³	4.8e ³	1.1e ¹	6.1e ²	8.9e ¹
	1.4	1.2e ³	4.4	3.3	6.5e ²	5.5e ²	8.4	1.5e ³	5.7e ¹
	7.2	6.2e ²	7.5e ¹	1.2	1.2e ²	1.4	1.5	1.2e ³	2.6

According to Table I and Section III, in the case of the fault there is decaying dc at least in two phases while there is no decaying dc during power swing. Therefore, in order to detect fault during power swing, current waveform components are calculated using Prony method. If the decaying dc amplitude is among the two first biggest amplitudes for three successive windows, three-phase fault has happened and the relay should be unblocked. In this case three-phase fault is detected after 4.7 ms (0.3 cycle) and relay is unblocked.

TABLE III
CURRENT WAVEFORM COMPONENTS DURING DIFFERENT THREE PHASE FAULTS

case	Z line (Ω/km)	X/R for Z1 and Z0	Zf (Ω)	X% of transfor mer	Fault location (km)	Fault inception (sec)	Ia			Ib			Ic		
							Amplitude	Frequency	Damping	Amplitude	Frequency	Damping	Amplitude	Frequency	Damping
1	Z1=0.12+0.88i Z0=0.309+1.297i	7.3 4.2	25	12%	15	1	4.1e ³	0	1.3e ²	3e ³	6.3 e ¹	6.2	4.8e ³	0	1.9e ²
							3e ³	6.2e ¹	3.2	5.2e ¹	0	5.1e ³	3.5e ³	6.3 e ¹	7.9e ⁻¹
2	Z1=0.12+1.09i Z0=0.309+1.85i	9 6	20	15%	30	1.1	3.2e ³	6.2e ¹	5.6	3e ³	6.3 e ¹	6.8	3.2e ³	6.3 e ¹	1.1e ¹
							5.1e ²	0	2.1e ⁵	1.7e ³	0	1.3e ²	2.1e ³	0	1.7e ²
3	Z1=0.14+1.54i Z0=0.35+1.75i	11 5	15	20%	40	1.03	2.8e ³	6.0e ¹	9.5	3.9e ³	0	1.2e ²	4.5e ³	0	8.9e ¹
							3.1e ²	7.2e ²	1.1e ²	2.8e ³	6.0e ¹	1.3e ¹	2.7e ³	6.0e ¹	8.7
4	Z1=0.14+1.12i Z0=0.35+1.75i	8 5	10	10%	70	1.02	5.2e ³	6.0e ¹	5.4e ¹	5.7e ²	0	1.1e ⁴	6.8e ²	0	8.5e ³
							3.7e ²	0	2.1e ²	4.4e ¹	6.0e ¹	1.1e ¹	1.2e ²	6.1e ¹	1.3e ¹
5	Z1=0.17+1.7i Z0=0.4+2.8i	10 7	5	15%	100	1.07	5.2e ³	0	1.9e ³	2.4e ³	6.2e ¹	2.4e ²	1.9e ³	6.3e ¹	2.7e ²
							2.4e ³	5.8e ¹	1.0e ²	7.2e ²	4.4e ²	1.2e ³	9.7e ²	0	1.1e ¹
6	Z1=0.12+0.79i Z0=0.31+1.24i	6.5 4	0	20%	120	1.09	2.1e ³	6.3e ¹	1.0e ²	3.9e ³	0	2.3e ⁴	2.6e ³	6.0e ¹	9.1e ¹
							7.5e ¹	0	8.4e ³	1.2e ¹	5.9e ¹	1.0e ¹	6.8e ²	0	1.8e ⁴
							6.6	3.1e ³	8.1e ³	6.7	2.0e ³	2.8e ³	3.5e ¹	5.0e ²	1.5e ³

In the second case, a three-phase fault that includes arc is considered. Arc has been modeled according to [25]. The dynamic arc characteristics are simulated by the following equation:

$$\frac{dg}{dt} = \frac{1}{T}(G - g) \quad (13)$$

where g is the time varying arc conductance, and T is the time constant, which is calculated as follows:

$$T = \frac{\alpha \times I}{l} \quad (14)$$

where the coefficient α is about 2.85×10^{-5} and I is peak value of arc current, and l is the arc length. G is the stationary primary arc conductance calculated as follows:

$$G = \frac{|i|}{V \times l} \quad (15)$$

$|i|$ absolute value of arc current;

V constant voltage parameter per unit length of primary arc, which is about 15 V/cm over the range of current 1.4 kA to 24 kA.

Fig. 11 shows currents due to three-phase fault while arc with length of 4.5 m is included and happens at 1.0084 s. Amplitude of decaying dc versus time of phase b has been shown in Fig. 12. Current waveform components during one window data have been given in Table II.

In this case three-phase fault is detected after 5.6 ms (0.34 cycle) and relay is unblocked.

Table III shows the current waveform components of different fault cases at different locations, inceptions, impedance values (Zf), and source impedances (Zs).

As Tables I–III show, there is a decaying dc during the three-phase fault at least in two phases, while it is not so during the power swing. As mentioned before, sensing decaying dc component of current waveform can be a suitable property for detecting fault during the power swing.

As discussed in Section III, the proposed method should not be used stand alone. In fact the goal of the proposed method is supervising the existing simple fault detection methods which work properly in asymmetrical faults but fail to work in symmetrical faults. For instance negative sequence component-based methods explained in Section I are powerful, simple and widely used methods in power system relaying. However, they fail to operate in the case of occurrence of symmetrical faults. The proposed method can be added to supervise them in the case of symmetrical faults.

The fact that the proposed method is based on detecting presence of decaying dc in current waveform, not calculating exact amount, makes it able to detect symmetrical fault from power swing very fast. If the proposed method was based on calculating exact amount of decaying dc, (for instance there was a predefined value that should have reached) it would impose extra delay to the algorithm. The proposed method is based on relative presence of decaying dc in current waveform which makes it possible to detect symmetrical faults in fraction of a cycle as demonstrated in simulation results. Therefore it operates properly even in the fault cases with fast decaying dc components.

V. CONCLUSION

This paper introduced a new method for detecting three-phase fault during the power swing, which may be used for unblocking the distance relay. This method is based on the presence of decaying dc component in the current waveform as a sign of the fault occurrence. The use of this method improves distance relay

dependability by unblocking it during power swing if a fault occurs at the same time.

The merit of the proposed method was demonstrated by simulating various cases including solid faults and arc fault on a typical power system. The ease of implementation as well as accuracy and high speed of fault detection are important advantages of the proposed method.

REFERENCES

[1] N. Zhang and M. Kezunovic, "A study of synchronized sampling based fault location algorithm performance under power swing and out-of-step conditions," in *Proc. PowerTech*, St. Petersburg, Russia, Jun. 2005, pp. 1–7.

[2] P. J. Moore and A. T. Johns, "New method of power swing blocking for digital distance protection," *Proc. Inst. Elect. Eng., Gen., Transm. Distrib.*, vol. 143, no. 1, pp. 19–26, Jan. 1996.

[3] X. Lin, Y. Gao, and P. Liu, "A novel scheme to identify symmetrical faults occurring during power swings," *IEEE Trans. Power. Del.*, vol. 23, no. 1, pp. 73–78, Jan. 2008.

[4] S. Jiao, Z. Bo, W. Liu, and Q. Yang, "New principles to detect faults during power swing," in *Proc. Inst. Elect. Eng., Developments in Power System Protection 7th Int. Conf.*, Amsterdam, The Netherlands, 2001, pp. 515–518.

[5] B. Su, X. Z. Dong, Z. Q. Bo, Y. Z. Sun, B. R. J. Counce, D. Tholomier, and A. Apostolov, "Fast detector of symmetrical fault during power swing for distance relay," in *Proc. Power Eng. Soc. General Meeting*, San Francisco, CA, Jun. 2005, vol. 2, pp. 1836–841.

[6] G. Benmouyal, D. Hou, and D. Tziouvaras, "Zero-setting power-swing blocking protection," presented at the 31st Annu. Western Protective Relay Conf., Spokane, WA, Oct. 2004.

[7] A. Mechraoui and D. W. P. Thomas, "A new blocking principle with phase and earth fault detection during fast power swings for distance protection," *IEEE Trans. Power. Del.*, vol. 10, no. 3, pp. 1242–1248, Jul. 1995.

[8] A. Mechraoui and D. W. P. Thomas, "A new principle for high resistance earth fault detection during fast power swings for distance protection," *IEEE Trans. Power. Del.*, vol. 12, no. 4, pp. 1452–1457, Oct. 1997.

[9] S. M. Brahma, "Distance relay with out-of-step blocking function using wavelet transform," *IEEE Trans. Power. Del.*, vol. 22, no. 3, pp. 1360–1366, Jul. 2007.

[10] H. K. Zadeh and Z. Li, "A novel power swing blocking scheme using adaptive neuro-fuzzy inference system," *Electric Power Syst. Res.*, vol. 78, pp. 1138–1146, 2008.

[11] J. Faiz and S. Lotfi-Fard, "A novel wavelet-based algorithm for discrimination of internal faults from magnetizing inrush currents in power transformers," *IEEE Trans. Power. Del.*, vol. 21, no. 4, pp. 1989–1996, Oct. 2006.

[12] N. Zhang and M. Kezunovic, "Transmission line boundary protection using wavelet transform and neural network," *IEEE Trans. Power. Del.*, vol. 22, no. 2, pp. 859–869, Apr. 2007.

[13] J. Faiz, S. Lotfi-fard, and S. Haidarian Shahri, "Prony-based optimal bayes fault classification of over-current protection," *IEEE Trans. Power. Del.*, vol. 22, no. 3, pp. 1326–1334, Jul. 2007.

[14] M. M. Tawfik and M. M. Morcos, "On the use of Prony method to locate fault in loop system by utilizing modal parameters of fault current," *IEEE Trans. Power Del.*, vol. 20, no. 1, pp. 532–534, Jan. 2005.

[15] M. M. Tawfik and M. M. Morcos, "ANN-based techniques for estimating fault location on transmission line using Prony method," *IEEE Trans. Power Del.*, vol. 16, no. 2, pp. 219–224, Apr. 2001.

[16] T. Lobos, J. Rezmer, and H. J. Koglin, "Analysis of power system transients using wavelet and Prony method," presented at the IEEE Power Tech Conf., Porto, Portugal, Sep. 2001.

[17] A. T. Johns and S. K. Salman, *Digital Protection for Power Systems*. London, U.K.: Peregrinus, 1995.

[18] H. M. Tran and H. Akyea, "Numerical Distance Protection Relay Commissioning and Testing," M.Sc thesis, Chalmers Univ. Technol. Goteborg, Goteborg, Sweden, Oct. 2005.

[19] X. Luo and M. Kezunovic, "A novel digital relay model based on SIMULINK and its validation based on expert system," in *Proc. Transmission and Distribution Conf. Exhibit.: Asia and Pacific*, 2005, pp. 1–6.

[20] Q. Q. Xu, J. Suonan, and Y. Z. Ge, "Real-time measurement of mean frequency in two-machine system during power swings," *IEEE Trans. Power. Del.*, vol. 19, no. 3, pp. 1018–1023, Jul. 2004.

[21] L. V. Der Siuis, *Transients in Power Systems*. New York: Wiley, 2001.

[22] K. Malmedal and P. K. Sen, "Arcing faults and their effect on the settings of ground fault relays in solidly grounded low voltage systems," presented at the North American Power Symp., Cleveland, OH, Oct. 1998.

[23] A. Gaudreau and B. Koch, "Evaluation of LV and MV arc parameters," *IEEE Trans. Power. Del.*, vol. 23, no. 1, pp. 487–492, Jan. 2008.

[24] V. Balamourougan and T. S. Sidhu, "A new filtering technique to eliminate decaying DC and harmonics for power system phasor estimation," in *Proc. Power India Conf.*, India, Apr. 2006, pp. 1–5.

[25] A. T. Johns, R. K. Aggarwal, and Y. H. Song, "Improved techniques for modeling fault arcs on faulted EHV transmission systems," *Proc. Inst. Elect. Eng., Gen., Transm. Distrib.*, vol. 141, no. 2, pp. 148–154, Mar. 1994.



Saeed Lotfifard (S'08) was born in Karaj, Iran, in 1982. He received the B.Sc. and M.Sc. degrees in electrical engineering in 2004 and 2006, respectively, and is currently pursuing the Ph.D. degree in electrical and computer engineering at Texas A&M University.

His research interests are power system protection, power-quality analysis, signal processing, and its application to transients and protection of power systems.



Jawad Faiz (M'90–SM'93) received the Bachelor and Master's (Hons.) degrees in electrical engineering from the University of Tabriz, Tabriz, Iran, in 1974 and 1975, respectively, and the Ph.D. degree in electrical engineering from the University of Newcastle-upon-Tyne, Newcastle-upon-Tyne, U.K., in 1988.

Early in his career, he was a faculty member with the University of Tabriz for ten years. After he received the Ph.D. degree, he rejoined the University of Tabriz. Since 1999, he has been a Professor at the School of Electrical and Computer Engineering, Faculty of Engineering, University of Tehran, Tehran, Iran. His teaching and research interests are switched reluctance and VR motors design, design and modeling of electrical machines, drives, and transformers.

Dr. Faiz is a member of the Iran Academy of Science.



Mladen Kezunovic (S'77–M'80–SM'85–F'99) received the Dipl.Ing. degree from the University of Sarajevo in 1974, and the M.S. and Ph.D. degrees in electrical engineering from the University of Kansas in 1977 and 1980, respectively.

Currently, he is the Eugene E. Webb Professor and Site Director of the Power Engineering Research Center (PSerc), an NSF IUCRC at Texas A&M University, College Station. He was with Westinghouse Electric Corp., Pittsburgh, PA, from 1979 to 1980 and the Energoinvest Co., Europe, from 1980 to 1986. He spent a sabbatical at EdF, Clamart, France, from 1999 to 2000. He was also a Visiting Professor at Washington State University, Pullman, from 1986 to 1987 and The University of Hong Kong in 2007. His main research interests are digital simulators and simulation methods for relay testing as well as the application of intelligent methods to power system monitoring, control, and protection.

Dr. Kezunovic is a member of CIGRE and a Registered Professional Engineer in Texas.